2007CEAB...31..187T

ISSN 1845–8319

ANALYSIS OF THE FLARE WAVE ASSOCIATED WITH THE 3B/X3.8 FLARE OF JANUARY 17, 2005

J. K. THALMANN[1], A. M. VERONIG[1], M. TEMMER[2], B. VRŠNAK[2] and A. HANSLMEIER[1]

[1]*IGAM, Institute of Physics, University of Graz, Universitätsplatz 5, A–8010 Graz, Austria*
[2]*Hvar Observatory, Faculty of Geodesy, University of Zagreb, Kačićeva 26, HR–10000 Zagreb, Croatia*

Abstract. The flare wave associated with the 3B/X3.8 flare and coronal mass ejection (CME) of January 17, 2005 are studied using imaging data in the Hα and EUV spectral channels. Due to the high-cadence Hα observations from Kanzelhöhe Solar Observatory (KSO), a distinct Moreton wave can be identified in $\sim$40 Hα frames over a period of $\sim$7 minutes. The associated coronal EIT wave is identifiable in only one EUV frame and appears close to the simultaneously observed Moreton wave front, indicating that they are closely associated phenomena. Beside the morphology of the wave across the solar disc (covering an angular extend of $\sim$130°), the evolution in different directions is studied to analyse the influence of a coronal hole (CH) on the wave propagation. The Moreton wave shows a decelerating character which can be interpreted in terms of a freely propagating fast-mode MHD shock. The parts of the wave front moving towards the CH show a lower initial and mean speed, and a greater amount of deceleration than the segments moving into the undisturbed direction. This is interpreted as the tendency of high Alfvén velocity regions to influence the propagation of wave packets.

Key words: shock waves - chromosphere - corona - flares

1. Introduction

Explosive processes in the solar atmosphere such as flares and CMEs launch shock waves into the solar atmosphere visible as wave-like phenomena propagating across the solar disk as well as through the corona. Such disturbances were recognized first in the 1960s in the chromospheric Hα spectral line (Moreton and Ramsey, 1960; Athay and Moreton, 1961). The overall appearance of these so-called Moreton waves is in form of diffuse arcs spangled with more intense localized brightenings. Propagating away from the source region the former diffuse leading edges become less intense but more

Hvar Observatory, Faculty of Geodesy • Provided by the NASA Astrophysics Data System

2007CEAB...31..187T

sharp (see Warmuth *et al.*, 2004). They are often accompanied by type II radio bursts which had already been interpreted to be excited by fast-mode magnetohydrodynamic (MHD) shocks in the solar corona (Uchida, 1960). Uchida (1968, 1970) developed a theoretical interpretation in which the intersection of a fast-mode coronal wavefront with the chromosphere sweeps along the chromosphere and corresponds to the observed Moreton disturbance. The Moreton waves are propagating with velocities of order $10^3\,\mathrm{km\,s^{-1}}$ visible over distances up to 10^6 km. Moreton waves are emitted into non-magnetic or weak-field regions by flares which occur at the edges of the magnetic regions and are usually confined within a sector angle of $\sim 90^\circ$ (Uchida *et al.*, 1973). High Alfvén velocity regions (e.g. sunspots and CHs) tend to reflect wave packets, while low Alfvén velocity regions tend to attract them (Uchida, 1970; Uchida *et al.*, 1973).

In the end of the 1990s coronal wave-like disturbances became observable in the EUV spectral band with the SoHO/EIT instrument (Delaboudiniere *et al.*, 1995) and are therefore referred to as EIT waves (Moses *et al.*, 1997; Thompson *et al.*, 1999). Due to the availability of coronal imaging data assumptions have been made that the Moreton waves could be the chromospheric counterpart of the coronal EIT waves (supporting Uchida's counterpart theory). However, this does not need to be true because Moreton waves seem to propagate between two or three times faster than EIT waves (Klassen *et al.*, 2000). Furthermore, EIT waves can be traced to larger distances than Moreton waves, but are observed only at the low time cadence of EIT ($\sim$12 min). This discrepancy might be due to a possible deceleration caused by a decreasing shock amplitude of the Moreton waves (Vršnak and Lulić, 2000a,b) which are visible only during the early phase of propagation, resulting in a close association observed between EIT and Moreton waves in certain cases (Thompson *et al.*, 1999, 2000; Warmuth *et al.*, 2001; Khan and Aurass, 2002; Okamoto *et al.*, 2004; Warmuth *et al.*, 2004; Vršnak *et al.*, 2006). On the other hand, Eto *et al.* (2002) found that a certain class of EIT waves ('diffuse' EIT waves) are certainly not a coronal counterpart of Moreton waves. However, another class ('sharp' EIT waves) may probably represent such a counterpart.

Despite these clear results, it has to be noted that Moreton waves are comparatively rare phenomena since their occurrence rate is much lower than that of both EIT waves and type II bursts. Probable reasons are that propagating coronal disturbances with low amplitudes are too weak to pro-

Hvar Observatory, Faculty of Geodesy • Provided by the NASA Astrophysics Data System

2007CEAB...31..187T

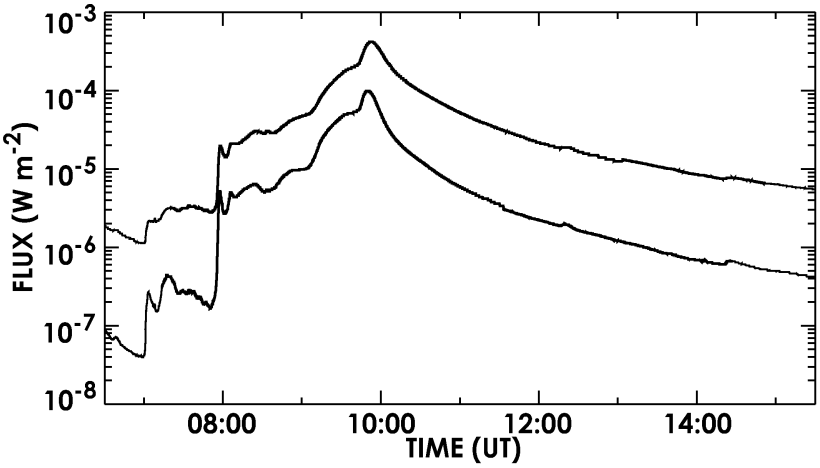

Figure 1: GOES 0.5–4 Å and 1–8 Å flux of the January 17, 2005 3B/X3.8 flare.

duce corresponding chromospheric signatures, or that there exists a class of EIT perturbations which is not associated with flare waves at all (for a review see Vršnak, 2005; Warmuth, 2006).

2. Data and Observations

The 3B/X3.8 flare on January 17, 2005 was produced by Active Region NOAA 10720 (N13/W25). It was a large and complex sunspot group consisting of 37 spots and spanning a length of $\sim$15°. The magnetic configuration of the spots classified by the Mt. Wilson system was $\beta\gamma\delta$. The largest flare produced by the region was an X3.8 flare which peaked around 09:47 UT. The evolution of the flare is complex and consists of several stages. Around 08:00 UT the GOES flux shows a sudden increase to M2 level and then increases gradually for about 100 min to X2 level . Due to a final enhancement at $\sim$09:40 UT the X4 peak is reached at $\sim$09:50 UT (Figure 1). The Moreton disturbance is associated with this last peak. The flare evolution as observed in Hα + 0.4 Å shows the flaring region close to the sunspots of AR 10720 before 09:40 UT. Images from the SoHO/EIT instrument show beside coronal wave signatures a CH at the solar north pole which lies in the direction of the propagation of the northern flank of the wave.

Flare wave signatures were detected and studied in the line centre, the red wing (Hα + 0.4 Å), and the blue wing (Hα − 0.3 Å) of the Hα spectral line. This chromospheric imaging data was available in form of high cadence

Hvar Observatory, Faculty of Geodesy • Provided by the NASA Astrophysics Data System

2007CEAB...31..187T

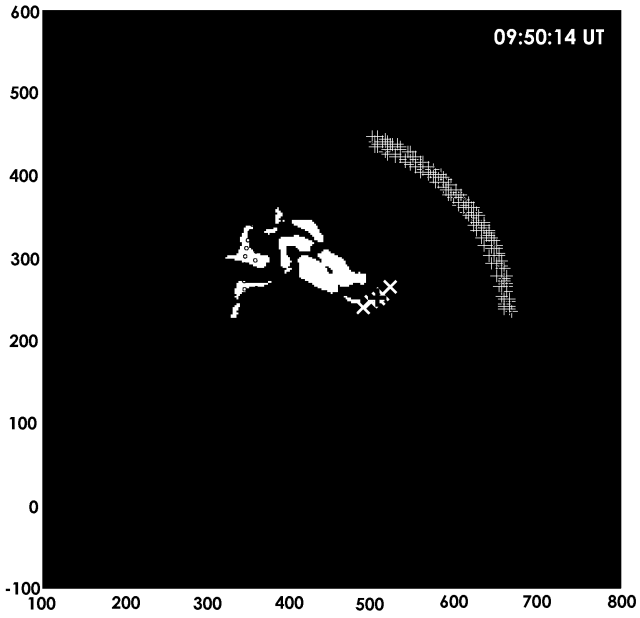

Figure 2: Hα + 0.4 Å full-disk image as observed at 09:50:14 UT. The leading edge (white plus signs) of the first visible wavefront as observed in running-difference images is visually determined five times. Superposed are the fitted ellipses (black) used for calculating the rough starting locations (white crosses). The mean value (black plus sign) is the estimated starting point of the disturbances. Units are arcsec from Sun centre, the field of view is $700'' \times 700''$.

full-disk images observed at KSO. Additionally, coronal data were available as Fe XII (195 Å) full-disk images recorded by the SoHO/EIT instrument.

3. Results

Altogether, 27 wave fronts were identified in running-difference images of the Hα line centre frames, six in the Hα red wing and five in the Hα blue wing images spanning a maximum angle of $\sim$130° (Figure 3). The wave fronts were observed in the time range from 09:43:25 UT to 09:50:38 UT and showed up for the first time at a distance of $\sim$120 Mm off the flare and can be traced up to $\sim$500 Mm away from the flaring region. Only one single wave front was visible in the EIT images at 09:46:55 UT due to the low time cadence of the SoHO/EIT instrument ($\sim$12 min). One frame later, the EIT wave already passed the visible hemisphere.

The Moreton wave ignition site was estimated by applying circular fits to the earliest observed Hα wave front, whereby the projection effect due to the spherical solar surface was taken into account (following Warmuth *et al.*,

Hvar Observatory, Faculty of Geodesy • Provided by the NASA Astrophysics Data System

2007CEAB...31..187T

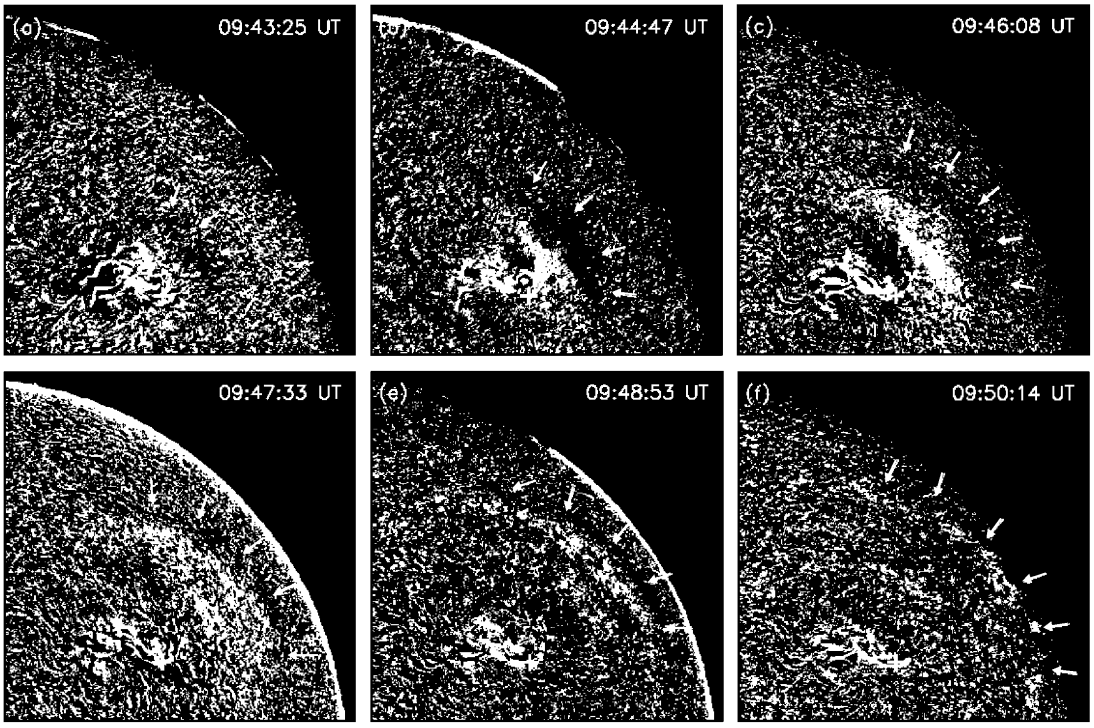

Figure 3: Sequence of Hα + 0.4 Å running-difference images. The leading edges of the Moreton wave fronts are seen as dark fronts (indicated by white arrows) which are followed by a bright wake. The field of view is $900'' \times 900''$.

2004). By this method we find the wave ignition centre at $x \approx 505'' \pm 13''$ and $y \approx 252'' \pm 10''$, which is outside the strong sunspots of the active region (Figure 2). For each point of the wave front, the distance from the ignition site was measured along great circles on the solar surface. The corresponding distance-time diagram (Figure 4) shows for each instant the mean value derived from the distances of all points on one wave front together with the standard deviation (error bars).

To analyse the kinematics of the wave, a linear and quadratic least-squares fit was calculated taking every distance point into account. A restriction was made by neglecting the first visible wave front in the red (Hα + 0.4 Å) wing at 09:43:25 UT because it was very diffuse and thus uncertain to measure. From the linear fit (i.e. assuming a uniform motion), we find the starting time to be 09:41:20 UT ± 20 s which well corresponds to the last enhancement of the GOES flux around 09:40 UT (Figure 1). The mean speed of the wave propagation is 910 ± 20 km s^{-1}. The quadratic fit (i.e. assuming a constantly accelerated motion) gives for the starting time

Hvar Observatory, Faculty of Geodesy • Provided by the NASA Astrophysics Data System

2007CEAB...31..187T

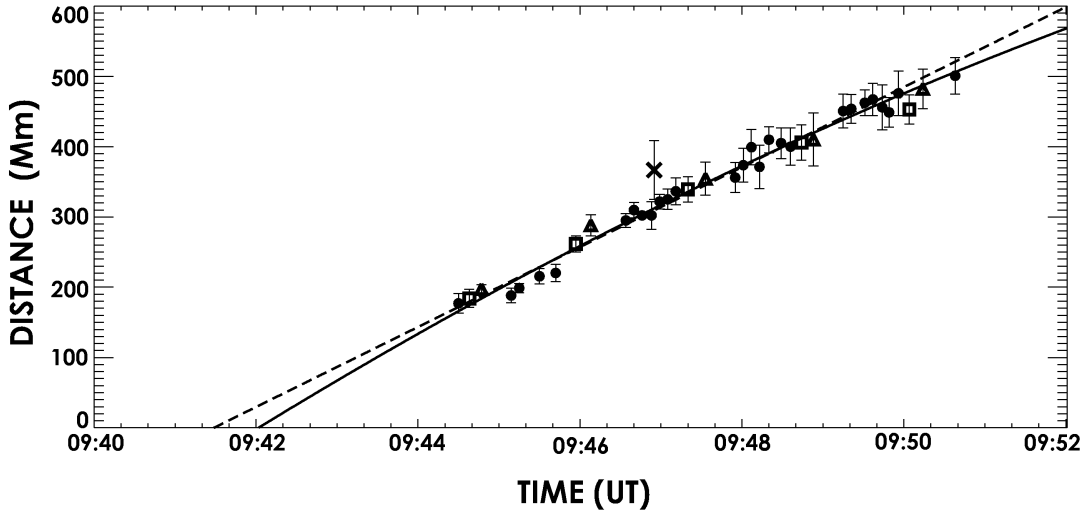

Figure 4: Distance-time diagram. At each instant the mean value derived from all points on the measured Hα (dots), Hα + 0.4 Å (triangles), Hα − 0.3 Å (squares) and EIT (cross) wave fronts is plotted. Superposed are the results form a linear (dashed line) and quadratic (solid line) least-squares fit to the data.

09:42:10 UT ± 30 s, an initial speed of 1280 ± 70 km s^{-1}, and a significant deceleration of −1150 ± 390 m s^{-2}.

The distance derived from the EIT wave shows up ∼50 Mm ahead of the kinematic curve of the Moreton wave but is roughly on the same kinematic curve. This is in contrast to the statistical result that EIT waves are significantly slower than Moreton waves (Klassen *et al.*, 2000) and agrees with Uchida's sweeping-skirt hypothesis.

Due to the large angular extent it was possible to investigate the Moreton wave propagation characteristics in different directions. It was found that the more the direction of propagation is oriented towards the solar north (i.e. towards the CH) the slower the wave front propagates. In early stages of the propagation the observed velocities are approximately equal in different directions, whereas they tend to differ remarkably at later stages. The last visible wave front in the westward direction is located ∼60 Mm farther away from the estimated ignition centre than the corresponding wave front segment moving towards the CH (Figure 5).

4. Summary and Conclusions

A Moreton and an EIT wave associated with a 3B/X3.8 flare have been studied. The Moreton wave signatures were detected in the centre and wings

Hvar Observatory, Faculty of Geodesy • Provided by the NASA Astrophysics Data System

2007CEAB...31..187T

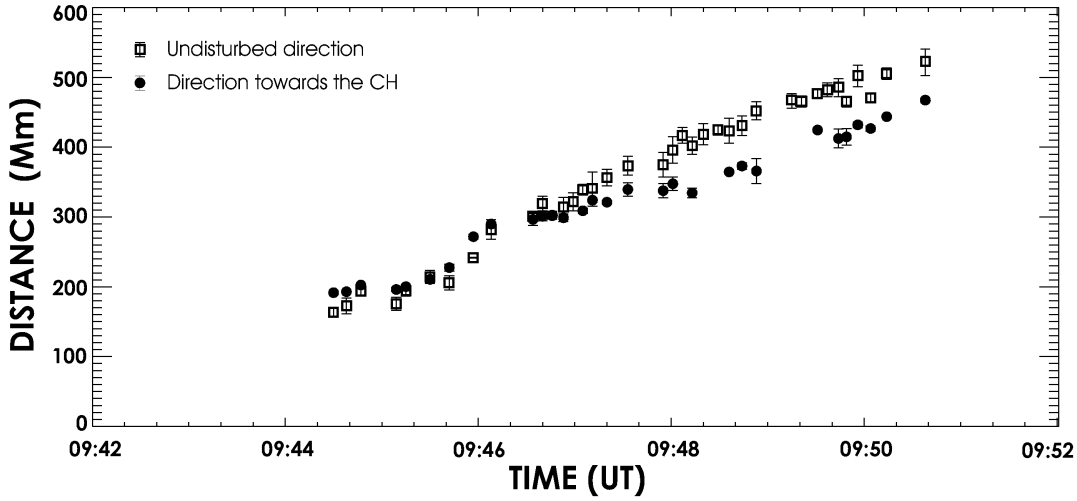

Figure 5: Distance-time diagram. Wave distances in the westward direction (squares) and in the direction of the northern CH (circles) with the corresponding standard deviations (error bars).

of the Hα spectral line in form of high cadence full-disk images observed at KSO. Additionally, one single EIT wave front was observed in SoHO/EIT full-disk images.

From analysing the distance-time diagram one could back-extrapolate the disturbances' starting time to ∼09:42 UT which corresponds well with the impulsive phase of the associated flare. Furthermore, the finding that the kinematics of all visually determined wave fronts shows a decelerating character suggests that they are not driven. This is expected for a propagating fast-mode MHD shock (blast wave) initially triggered by a flare (Vršnak and Lulić, 2000b). So far, the studied Moreton wave seems to be a consequence of an abrupt expansion of the flaring volume.

Wave fronts were identified in ∼40 running-difference images in the time range of ∼7 minutes, spanning a maximum angle of 130°. The first observed Moreton wave front is located ∼120 Mm off the estimated wave ignition centre. The disturbances are not observed in the closest neighbourhood of the flare which can be interpreted as the time/distance needed to build up a large amplitude wave or a shock wave.

Furthermore, the study of the Moreton wave's motion into different directions suggests that the perturbations' propagation is affected by a CH situated at the solar north – a high Alfvén velocity region which tends to reflect the wave fronts. In fact, the covered distances towards the CH are much lower (by ∼60 Mm) than those into the undisturbed direction (for detailed

Hvar Observatory, Faculty of Geodesy • Provided by the NASA Astrophysics Data System

2007CEAB...31..187T

analysis see Veronig *et al.*, 2006). A similar case was studied by Thompson *et al.* (1998) for the observable EIT wave of May 12, 1997 which stopped at the boundary of an existing CH.

References

Athay, R. G. and Moreton, G. E.: 1961, *Astrophys. J.* **133**, 935.

Delaboudiniere, J.-P., Artzner, G. E., Brunaud, J., and 25 coauthors: 1995, *Solar Phys.* **162**, 291.

Eto, S., Isobe, H., Narukage, N., Asai, A., Morimoto, T., Thompson, B., Yashiro, S., Wang, T., Kitai, R., Kurokawa, H., and Shibata, K.: 2002, *Publ. Astron. Soc. Jpn.* **54**, 481.

Khan, J. I. and Aurass, H.: 2002, *Astron. Astrophys.* **383**, 1018.

Klassen, A., Aurass, H., Mann, G., and Thompson, B. J.: 2000, *Astron. Astrophys., Suppl. Ser.* **141**, 357.

Moreton, G. E. and Ramsey, H. E.: 1960, *Publ. Astron. Soc. Pac.* **72**, 357.

Moses, D., Clette, F., and Delaboudiniere: 1997, *Solar Phys.* **175**, 571.

Okamoto, T. J., Nakai, H., Keiyama, A., Narukage, N., UeNo, S., Kitai, R., Kurokawa, H., and Shibata, K.: 2004, *Astrophys. J.* **608**, 1124.

Thompson, B. J., Gurman, J. B., Neupert, W. M., Newmark, J. S., Delaboudinière, J.-P., St. Cyr, O. C., Stezelberger, S., Dere, K. P., Howard, R. A., and Michels, D. J.: 1999, *Astrophys. J., Lett.* **517**, L151.

Thompson, B. J., Plunkett, S. P., Gurman, J. B., Newmark, J. S., St. Cyr, O. C., and Michels, D. J.: 1998, *Geophys. Res. Lett.* **25**, 2465.

Thompson, B. J., Reynolds, B., Aurass, H., Gopalswamy, N., Gurman, J. B., Hudson, H. S., Martin, S. F., and St. Cyr, O. C.: 2000, *Solar Phys.* **193**, 161.

Uchida, Y.: 1960, *Publ. Astron. Soc. Jpn.* **12**, 376.

Uchida, Y.: 1968, *Solar Phys.* **4**, 30.

Uchida, Y.: 1970, *Publ. Astron. Soc. Jpn.* **22**, 341.

Uchida, Y., Altschuler, M. D., and Newkirk, G. J.: 1973, *Solar Phys.* **28**, 495.

Veronig, A. M., Temmer, M., Vršnak, B., and Thalmann, J. K.: 2006, *Astrophys. J.* **647**, 1466.

Vršnak, B.: 2005, *EOS Transactions* **86**, 112.

Vršnak, B. and Lulić, S.: 2000a, *Solar Phys.* **196**, 157.

Vršnak, B. and Lulić, S.: 2000b, *Solar Phys.* **196**, 181.

Vršnak, B., Warmuth, A., Temmer, M., Veronig, A., Magdalenić, J., Hillaris, A., and Karlický, M.: 2006, *Astron. Astrophys.* **448**, 739.

Warmuth, A.: 2006, *Lecture notes — in preperation* .

Warmuth, A., Vršnak, B., Aurass, H., and Hanslmeier, A.: 2001, *Astrophys. J.* **560**, L105.

Warmuth, A., Vršnak, B., Magdalenić, J., Hanslmeier, A., and Otruba, W.: 2004, *Astron. Astrophys.* **418**, 1101.

Hvar Observatory, Faculty of Geodesy • Provided by the NASA Astrophysics Data System